Published in final edited form as:
Aerosol Sci Technol. 2012 March ; 46(3): 347–353. doi:10.1080/02786826.2011.631956.

The Structure of Agglomerates consisting of Polydisperse Particles

M.L. Eggersdorfer and **S.E. Pratsinis***
Particle Technology Laboratory, Institute of Process Engineering, Department of Mechanical and Process Engineering, ETH Zurich, Sonneggstrasse 3, CH-8092 Zürich, Switzerland

Abstract

Agglomeration is encountered in many natural or industrial processes, like growth of aerosol particles in the atmosphere and during material synthesis or even flocculation of suspensions, granulation, crystallization and with colloidal particle processing. These particles collide by different mechanisms and stick together forming irregular or fractal-like agglomerates. Typically, the structure of these agglomerates is characterized with the fractal dimension, D_f, and pre-exponential factor, k_n, of simulated agglomerates of monodisperse primary particles (PP) for ballistic or diffusion-limited particle-cluster and cluster-cluster collision mechanisms. Here, the effect of PP polydispersity on D_f and k_n is investigated with agglomerates consisting of 16 – 1024 PP with closely controlled size distribution (geometric standard deviation, σ_g = 1-3). These simulations are in excellent agreement with the classic structure (D_f and k_n) of agglomerates consisting of monodisperse PPs made by four different collision mechanisms as well as with agglomerates of bi-, tri-disperse and normally distributed PPs. Broadening the PP size distribution of agglomerates decreases monotonically their D_f and for sufficiently broad PP distributions (σ_g > 2.5) the D_f reaches about 1.5 and k_n about 1 regardless of collision mechanism. Furthermore with increasing PP polydispersity, the corresponding projected area exponent, D_a, and pre-exponential factor, k_a, decrease monotonically from their standard values for agglomerates with monodisperse PPs. So D_f as well as D_a and k_a can be an indication for PP polydispersity in mass–mobility and light scattering measurements, if the dominant agglomeration mechanism is known, like diffusion-limited and/or ballistic cluster-cluster coagulation in aerosols.

Keywords

aerosol physics; agglomerate; fractal dimension; polydisperse aerosol; morphology

Introduction

Significant advances have been made in agglomerate characterization by employing the so-called fractal theory and relating agglomerate structure to its generation pattern through the fractal dimension, D_f. For example, agglomerates made by diffusion-limited cluster-cluster agglomeration (DLCA) have D_f = 1.78 (Jullien et al. 1984) or by diffusion-limited particle-cluster agglomeration (DLA) have D_f = 2.5 (Tolman and Meakin 1989), ballistic cluster-cluster agglomeration (BCCA) have D_f = 1.90 (Meakin and Jullien 1988) and ballistic particle-cluster agglomeration (BPCA) have D_f = 3.0 (Ball and Witten 1984) as were summarized for aerosols by Schaefer and Hurd (1990). These D_f values have become the standard in agglomerate (physically-bound particles) and even aggregate (chemically- or

*Corresponding author: Ph. +41 (0) 44 632 31 80; Fax. +41 (0) 44 632 15 95, pratsinis@ptl.mavt.ethz.ch.
meggers@ptl.mavt.ethz.ch

Europe PMC Funders Author Manuscripts

sinter-bound particles) characterization despite the fact that such particles may not fully obey fractal theory but are sufficiently close to it to be called fractal-like.

This concept has served well process design of a wide spectrum of filamentary particles (carbon black, nickel and fumed silica), made mostly by aerosol coagulation. In fact, a number of characterization techniques and process design concepts have been developed capitalizing on these D_f values to extract other particle properties (e.g. collision diameter, primary particle size) and design reactors for manufacturing such particles. They are characterized by a power law relating the number of primary particles in an agglomerate to primary particle radius and radius of gyration or collision radius. For example, in aerosol reactor design, the coagulation rate of spherical particles is corrected to that of fractal-like ones in the free molecular (Matsoukas and Friedlander 1991) and continuum (Oh and Sorensen 1997) regimes by introducing the radius of gyration and D_f in their collision area term (Mountain et al. 1986).

What might have been overlooked in characterization and simulations of fractal-like particles is that the above D_f values have been developed for agglomerates of monodisperse primary particles. Notable exceptions come from Tence et al. (1986) and Bushell & Amal (1998) who had examined the effect of primary particle polydispersity on agglomerate structure and scattering behavior. They numerically generated BCCA and DLCA agglomerates having Gaussian-distributed (Tence et al. 1986) and mono-, bi- and tri-disperse (Bushell and Amal 1998) primary particles and found no effect on D_f for their employed polydispersities.

For coagulating aerosols, however, this needs to be carefully examined as Brownian coagulation-driven particle formation leads to polydisperse particles. Their distribution, even at a single streamline is, at best, as narrow as that given by self-preserving theory, e.g. having geometric standard deviation, σ_g, of about 1.45 (Landgrebe and Pratsinis 1989). When agglomerates are made in aerosol reactors at different (e.g. radial) residence time distributions and collected, typically, by filtration, much broader size distributions can be obtained. Agglomerates with quite polydisperse primary particle size distribution are obtained during gas-to-particle conversion or when primary particles with different residence time histories are mixed. So the common extraction of D_f by microscopic counting of such agglomerates and primary particles may not necessarily lead to an accurate assessment of their formation pathway as has been proposed by Schaefer and Hurd (1990). Similarly the use of D_f in designing aerosol synthesis of such particles needs to account for agglomerates of polydisperse primary particles.

Here fractal-like agglomerates consisting of 16, 64, 256, 512 and 1024 primary particles having closely controlled size distributions are generated by DLA, DLCA, BCCA and BPCA. So the employed primary particle radii are log-normally distributed with geometric standard deviation σ_g ranging from 1 (monodisperse) to 3 and the structure characteristics (D_f and pre-exponential factor k_n) of such agglomerates are calculated by fractal theory for these collision mechanisms and compared to the literature at limiting cases. Furthermore the projected area exponent and pre-exponential factor that are used in aerosol characterization by mass-mobility measurements are obtained as a function of primary particle polydispersity.

Theory

Agglomerates grown by particle collisions exhibit a power law scaling between number of primary particles, n_p, and radius of gyration, r_g (Mandelbrot 1982):

$$n_p = k_n \left(\frac{r_g}{r_p} \right)^{D_f}, \quad (1)$$

where the exponent D_f is the fractal dimension, r_p the monodisperse or geometric mean primary particle radius, k_n a prefactor and the radius of gyration is:

$$r_g^2 = \frac{\sum_i x_i^2 m_i}{\sum_i m_i}, \quad (2)$$

with m_i being the mass and x_i the distance of primary particle i to the agglomerate center of mass. For agglomerates of polydisperse primary particles, the equivalent monodisperse or surface area mean primary particle radius r_{va} and number n_{va} is commonly determined by the (total) agglomerate volume v and surface area a:

$$r_{va} = \frac{3v}{a}, \quad (3)$$

$$n_{va} = \frac{v}{4\pi r_{va}^3/3}, \quad (4)$$

This corresponds to the average primary particle radius determined experimentally by nitrogen adsorption, r_{BET}, and small angle X-ray scattering (SAXS), r_{VS} (Hyeon-Lee et al. 1998). The r_{va} is equal to r_p for agglomerates of monodisperse spherical primary particles.

The projected agglomerate area a_a onto a plane is also related to n_p by a power law (Medalia 1967):

$$n_p = k_a \left(\frac{a_a}{a_p} \right)^{D_a}, \quad (5)$$

where a_p is the projected area of a primary particle and D_a and k_a are the power law exponent and prefactor, respectively. The projected area is an important agglomerate property as it can be used to define the agglomerate mobility diameter, d_m, in the free molecular regime (Meakin 1988):

$$d_m = \sqrt{\frac{4a_a}{\pi}}. \quad (6)$$

This holds well even in the transition regime up to Knudsen number $Kn = 0.28$ (Rogak et al. 1993). Equations 5 and 6 are used to characterize agglomerates by mass-mobility measurements (Park et al. 2003).

The a_a is calculated by Monte-Carlo integration (Meakin 1988) and averaged over 50 homogeneously distributed random angles for each agglomerate. The D_f and k_n as well as D_a and k_a are obtained by ensemble averaging over agglomerates of different n_p (Eggersdorfer et al. 2010) and similarly to the evaluation of experiments (Sorensen et al. 1992). The D_f or D_a is determined from the slope of r_g or a_a versus the n_p or n_{va} in a double logarithmic plot, while the intersection with the y-axis is the logarithm of the prefactor k_n or k_a, respectively (Medalia 1967; Forrest and Witten 1979).

Results and Discussion

Validation

One hundred agglomerates of each number (n_p = 16-1024) and polydispersity (σ_g = 1-3) of primary particles (PP) are generated by DLA (Witten and Sander 1981), DLCA (Botet et al. 1984), BCCA (Tence et al. 1986) and BPCA (Sutherland 1966) to determine D_f and k_n by eq. 1 and D_a and k_a by eq. 5. Figure 1 shows typical images of agglomerates made with monodisperse primary particles (σ_g = 1) for DLA, DLCA, BCCA and BPCA similar to Schaefer and Hurd (1990). These agglomerates have D_f = 1.79 ± 0.03 (DLCA), 1.89 ± 0.03 (BCCA), 2.25 ± 0.02 (DLA) and 2.81 ± 0.03 (BPCA). The DLCA and BCCA values are in excellent agreement with Jullien et al. (1984) and Tence et al. (1986). The D_f of DLA and BPCA are slightly smaller than their asymptotic limits of 2.5 and 3 by Tolman and Meakin (1989) and Ball and Witten (1984), respectively. This is a finite size effect, as the D_f of small agglomerates is always lower than their asymptotic D_f (Meakin 1999). The k_n = 1.40 ± 0.12 for monodisperse DLCA agglomerates (Table 1) is consistent with Sorensen & Roberts (1997). The BCCA, DLA and BPCA agglomerates of monodisperse primary particles have k_n = 1.36 ± 0.1, 0.86 ± 0.04 and 0.46 ± 0.03 (Table 1, actual n_p & r_p).

Agglomerates with bi- and tri-disperse primary particles were made also by DLCA to compare to Bushell and Amal (1998). These agglomerates consist of primary particles of two and three distinct diameters, respectively. Their bi-disperse agglomerates with a PP radius ratio of 3:1 and about 4% of the large particles were calculated here to have D_f = 1.79 ± 0.03. Similarly their tri-disperse PP radius ratio of 5:3:1 with distributions of 1:18:81% and PP radius ratio of 5:2:1 with distributions of 10:60:30% were calculated here to have D_f = 1.77 ± 0.03 and 1.79 ± 0.03, respectively. All were in excellent agreement with Bushell and Amal (1998) who had reported D_f = 1.78 ± 0.03. Tence et al. (1986) obtained by BCCA agglomerates of primary particles having a Gaussian-like distribution (n = 2 and β = 5) that corresponds to a σ_g = 1.35. The present simulations with primary particles having this σ_g resulted in agglomerates that had a D_f = 1.91 ± 0.05, which is quite close to that of 1.89 ± 0.03 (Tence et al. 1986). These results validate the employed algorithms to address the structure of agglomerates having arbitrarily broad distributions of primary particles.

Effect of Primary Particle Polydispersity on Fractal Dimension & Prefactor

The primary particles are log-normally distributed with a geometric standard deviation σ_g = 1-3. Figure 2 shows a TEM-like image of 100 DLCA agglomerates consisting of 512 PPs with σ_g = 2.

Figure 3 shows close-up snapshots of randomly chosen agglomerates consisting of 1024 PPs of σ_g = 2 and 3 made by DLCA, BCCA, DLA and BPCA along with the corresponding D_f. The broader the PP size distribution and thus the larger the difference between PPs, the stringier and more open are the agglomerates having a lower D_f than the benchmark agglomerates of monodisperse PPs (Fig. 1). At σ_g = 3 all agglomerates look similar somehow, regardless of collision mechanism.

Figure 4a quantifies these pictures by showing the D_f of agglomerates as a function of their constituent PP size distribution from σ_g = 1 (monodisperse) to 3 for DLCA (circles), BCCA (squares), DLA (triangles) and BPCA (diamonds). The D_f decreases with increasing σ_g and for σ_g = 3 the different collision mechanisms converge to nearly the same $D_f \approx$ 1.5. Clearly the presence of various primary particle sizes results in more open agglomerate structures. The more polydisperse are the PPs, the more open space leave between them within an agglomerate.

Polydispersity adds another element of disorder when uniform primary particles are replaced with non-uniform ones. As the motion of particles or clusters is independent from each other, their arrival or sticking point upon collision is fixed. Take for example particle-cluster agglomeration. The trajectory of the particle till its collision with a cluster is determined by its mobility diameter. As individual polydisperse PP arrive at the cluster, more irregular and open structures are developed than with uniform PPs. As a result, the compact agglomerate structures made by DLA and BPCA of monodisperse PPs with D_f of 2.25 and 2.81, respectively, are affected most dramatically by the PP polydispersity (Fig. 4a). Similar concepts apply to cluster-cluster agglomeration. The larger particles contribute much more to r_g than the smaller ones since r_g is calculated with the mass-weighted mean square displacement (eq. 2). So the D_f is very sensitive to PP polydispersity. The differences between particle masses increase for increasing σ_g so that at high polydispersities fewer particles effectively contribute to D_f. This results in $D_f = 1$ in the limit of two effective particles as r_g represents the high order moments of the distribution (square root of ratio between 2^{nd} and 0^{th} moment of mass-based distribution).

Figure 4a shows also the DLCA simulations (filled circles) of bi- and tri-disperse PPs by Bushell and Amal (1998) as well as the BCCA ones (filled square) of Tence et al. (1986). Clearly both studies had been carried out with relatively narrow PP size distributions to observe any reduction of D_f by the polydispersity of primary particles seen here. This monotonic reduction of D_f with increasing σ_g can be used to determine the effect of PP polydispersity on the structure of agglomerates by all four collision mechanisms.

Figure 4b shows the prefactor k_n for the agglomerates made here as a function of PP σ_g also. While the D_f decreases monotonically for increasing σ_g, regardless of collision mechanism, not all k_n exhibit such a monotonic behaviour. Nevertheless all reach a $k_n \approx 1$ for very broad PP polydispersities ($\sigma_g > 2.5$). For DLCA and BCCA particles, the k_n decreases continuously with increasing PP polydispersity, while for both DLA and BPCA k_n reaches a minimum here at $\sigma_g = 1.6$ and 1.5, respectively.

For $\sigma_g = 1.45$, the standard deviation of the self-preserving size distribution (SPSD) obtained by Brownian coagulation that corresponds best to DLCA, both D_f and k_n are within the error bars of agglomerates with monodisperse PPs and thus indistinguishable from each other. This indicates that PP polydispersity may not affect the structure of DLCA agglomerates made by aerosol coagulation on a single process streamline or residence time history. When, however, such particles are collected from a filter where particles of various residence time (and even temperature) histories are arriving, there would be a significant effect depending on their actual polydispersity. In practical systems, the primary particle size distribution is often unknown and for simplicity assumed to be monodisperse.

Table 1 compares the D_f and k_n determined with the actual r_p and n_p to that determined by the assumption of an average PP size of polydisperse ($\sigma_g = 1$-3) PPs using r_{va} and n_{va} as might be determined by microscopic counting, nitrogen adsorption or SAXS. For all agglomeration mechanisms, the D_f is not affected by more than 10%. In contrast, the k_n is overestimated significantly when assuming all primaries to have the same size for all collision mechanisms (Table 1, last column).

Effect of Primary Particle Polydispersity on Projected Surface Area & Mass-Mobility Characterization

The projected surface area a_a of agglomerates controls the mass and heat transfer, e.g. the collision frequency with particles much smaller than the gas mean free path and thus the mobility of agglomerates in the free molecular and transition regime (Meakin 1988; Rogak et al. 1993). For DLCA agglomerates of monodisperse PPs, $D_a = 1.08 \pm 0.002$ in Eq. 5,

consistent with Pierce et al. (2006). Similar to D_f, the D_a decreases with increasing σ_g (Fig. 5a). The a_a depends on the square of PP radius. So the largest PPs dominate while the smallest PPs hardly contribute to a_a. Agglomerates of the same mean PP radius but broader σ_g have also a larger a_a and in turn a reduced D_a regardless of collision mechanism.

Figure 5b shows the prefactor k_a of eq. 5 as a function of σ_g. The k_a decreases until $\sigma_g = 2.0$ and levels off for higher polydispersities. Though even for $\sigma_g = 3.0$, where D_f and k_n are nearly independent of collision mechanism indicating a similar mass distribution of the agglomerates, D_a and k_a differ for the four collision types. The DLCA particles have always the largest k_a and smallest D_a, since their most open structure results in primary particles that are less shielded by neighbors compared to BCCA, DLA and BPCA agglomerates (Fig. 1 & 3). For all collision mechanisms, the monotonic dependence of D_a and k_a on σ_g can be used to extract the effect of PP polydispersity of agglomerates by mass-mobility measurements as with D_f (Fig. 4a).

As two measures of fractal dimension are available for these agglomerates of various PP polydispersities and collision mechanisms, it is worth comparing them. So Figure 6 shows the D_f vs. $2D_a$ by combining Fig. 4a and 5a. For both diffusion-limited and ballistic cluster-cluster agglomeration, the r_g-based D_f is smaller than the r_m-based $2D_a$ regardless of PP polydispersity, with $r_m = d_m/2$. This is not surprising as DLCA and BPCA agglomerates have a $D_f < 2$ and very open chain-like structures even for a monodisperse PP size distribution, so always $r_m < r_g$ (Sorensen 2011) and $D_f < 2D_a$. Particle-cluster agglomerates (triangles & diamonds), however, are rather compact at $\sigma_g < 2$ with $D_f > 2$ (Fig. 4a) so $D_f > 2D_a$. Both BPCA and DLA agglomerates of monodisperse PPs have $r_m > r_g$ similar to that of a sphere with $r_m/r_g = \sqrt{5/3}$ (Hiemenz 1986). With increasing PP polydispersity, however, the particle-cluster agglomerates become more open so $r_m/r_g < \sqrt{5/3}$ and exhibit a transition at $D_f \approx 2.1$ from $D_f > 2D_a$ to $D_f < 2D_a$ (between $\sigma_g = 1.5$ and 2 in Fig. 4a & 5a) as their $r_m < r_g$. For $D_f > 2$, the projected areas are compact objects with screening of individual PP while for $D_f < 2$ almost all PPs are accessible (Mulholland et al. 1988). So the polydispersity of PPs affects most dramatically the structure of particle-cluster agglomeration made by both diffusion-limited and ballistic collisions.

Conclusions

Agglomerates consisting of polydisperse primary particles were generated by DLCA, BCCA, DLA and BPCA. The effect of primary particle size distribution on resulting agglomerate fractal dimension D_f and prefactor k_n, projected area exponent D_a and prefactor k_a was investigated. Asymptotic D_f and k_n values were obtained for agglomerates of primary particles having geometric standard deviation σ_g ranging from 1.0 to 3.0. These simulations were in agreement with the literature for fractal agglomerates of monodisperse primary particles and even with limited studies of fractal-like particles containing Gaussian-like, bi- and tri-disperse primary particles.

It was discovered that polydisperse primary particles result in more open agglomerate structures with lower D_f, D_a and k_a than the classic with monodisperse PPs. This is most notable for particle-cluster (up to 50% reduction) and to a lesser extent for cluster-cluster (up to 20% reduction) ballistic and diffusion-limited collision-generated agglomerates. Furthermore it was shown that the assumption of an average primary particle size, which is commonly applied in particle characterization, hardly affects D_f but significantly overestimates k_n for polydisperse PPs for all collision mechanisms. Most remarkably, for processes generating agglomerates by a known collision mechanism, a D_f, D_a or k_a smaller

than the benchmark values of agglomerates consisting of monodisperse PPs might be an indication for agglomerates of polydisperse primary particles.

Acknowledgments

Financial support by ETH Research Grant (ETHIIRA) ETH-11 09-1 and the European Research Council is gratefully acknowledged.

References

Ball RC, Witten TA. Causality bound on the density of aggregates. Phys. Rev. A. 1984; 29:2966–2967.

Botet R, Jullien R, Kolb M. Hierarchical model for irreversible kinetic cluster formation. J. Phys. A: Math. Gen. 1984; 17:L75–L79.

Bushell G, Amal R. Fractal aggregates of polydisperse particles. J. Colloid Interface Sci. 1998; 205:459–469. [PubMed: 9735210]

Eggersdorfer ML, Kadau D, Herrmann HJ, Pratsinis SE. Fragmentation and restructuring of soft-agglomerates under shear. J. Colloid Interface Sci. 2010; 342:261–268. [PubMed: 19948345]

Forrest SR, Witten TA. Long-range correlations in smoke-particle aggregates. J. Phys. A: Math. Gen. 1979; 12:L109–L117.

Hiemenz, PC. Principles of Colloid and Surface Chemistry. Marcel Dekker. Inc; New York: 1986.

Hyeon-Lee J, Beaucage G, Pratsinis SE, Vemury S. Fractal analysis of flame-synthesized nanostructured silica and titania powders using small-angle X-ray scattering. Langmuir. 1998; 14:5751–5756.

Jullien R, Kolb M, Botet R. Aggregation by kinetic clustering of clusters in dimensions d greater-than 2. J. Phys. Lett. 1984; 45:L211–L216.

Landgrebe JD, Pratsinis SE. Gas-phase manufacture of particulates - interplay of chemical-reaction and aerosol coagulation in the free-molecular regime. Ind. Eng. Chem. Res. 1989; 28:1474–1481.

Mandelbrot, BB. The fractal geometry of nature. W.H. Freeman; New York: 1982.

Matsoukas T, Friedlander SK. Dynamics of aerosol agglomerate formation. J. Colloid Interface Sci. 1991; 146:495–506.

Meakin P. Fractal aggregates. Adv. Colloid Interface Sci. 1988; 28:249–331. [PubMed: 2577851]

Meakin P. A historical introduction to computer models for fractal aggregates. J. Sol-Gel Sci. Technol. 1999; 15:97–117.

Meakin P, Jullien R. The effects of restructuring on the geometry of clusters formed by diffusion-limited, ballistic, and reaction-limited cluster cluster aggregation. J. Chem. Phys. 1988; 89:246–250.

Medalia AI. Morphology of aggregates .1. Calculation of shape and bulkiness factors - application to computer-simulated random flocs. J. Colloid Interface Sci. 1967; 24:393–404.

Mountain RD, Mulholland GW, Baum H. Simulation of aerosol agglomeration in the free molecular and continuum flow regimes. J. Colloid Interface Sci. 1986; 114:67–81.

Mulholland GW, Samson RJ, Mountain RD, Ernst MH. Cluster size distribution for free molecular agglomeration. Energy Fuels. 1988; 2:481–486.

Oh C, Sorensen CM. Light scattering study of fractal cluster aggregation near the free molecular regime. J. Aerosol Sci. 1997; 28:937–957.

Park K, Cao F, Kittelson DB, McMurry PH. Relationship between particle mass and mobility for diesel exhaust particles. Environ. Sci. Technol. 2003; 37:577–583. [PubMed: 12630475]

Pierce F, Sorensen CM, Chakrabarti A. Computer simulation of diffusion-limited cluster-cluster aggregation with an Epstein drag force. Phys. Rev. E. 2006:74.

Rogak SN, Flagan RC, Nguyen HV. The mobility and structure of aerosol agglomerates. Aerosol Sci. Technol. 1993; 18:25–47.

Schaefer DW, Hurd AJ. Growth and structure of combustion aerosols - fumed silica. Aerosol Sci. Technol. 1990; 12:876–890.

Sorensen CM. The Mobility of Fractal Aggregates: A Review. Aerosol Science and Technology. 2011; 45:765–779.

Sorensen CM, Cai J, Lu N. Light-scattering measurements of monomer size, monomers per aggregate, and fractal dimension for soot aggregates in flames. Appl. Opt. 1992; 31:6547–6557. [PubMed: 20733873]

Sorensen CM, Roberts GC. The prefactor of fractal aggregates. J. Colloid Interface Sci. 1997; 186:447–452. [PubMed: 9056374]

Sutherland DN. Comments on Vold's simulation of floc formation. J. Colloid Interface Sci. 1966; 22:300–302.

Tence M, Chevalier JP, Jullien R. On the measurement of the fractal dimension of aggregated particles by electron-microscopy - experimental-method, corrections and comparison with numerical-models. J. Phys. 1986; 47:1989–1998.

Tolman S, Meakin P. Off-lattice and hypercubic-lattice models for diffusion-limited aggregation in dimensionalities 2-8. Phys. Rev. A. 1989; 40:428–437. [PubMed: 9901909]

Witten TA, Sander LM. Diffusion-limited aggregation, a kinetic critical phenomenon. Phys. Rev. Lett. 1981; 47:1400–1403.

Europe PMC Funders Author Manuscripts

Europe PMC Funders Author Manuscripts

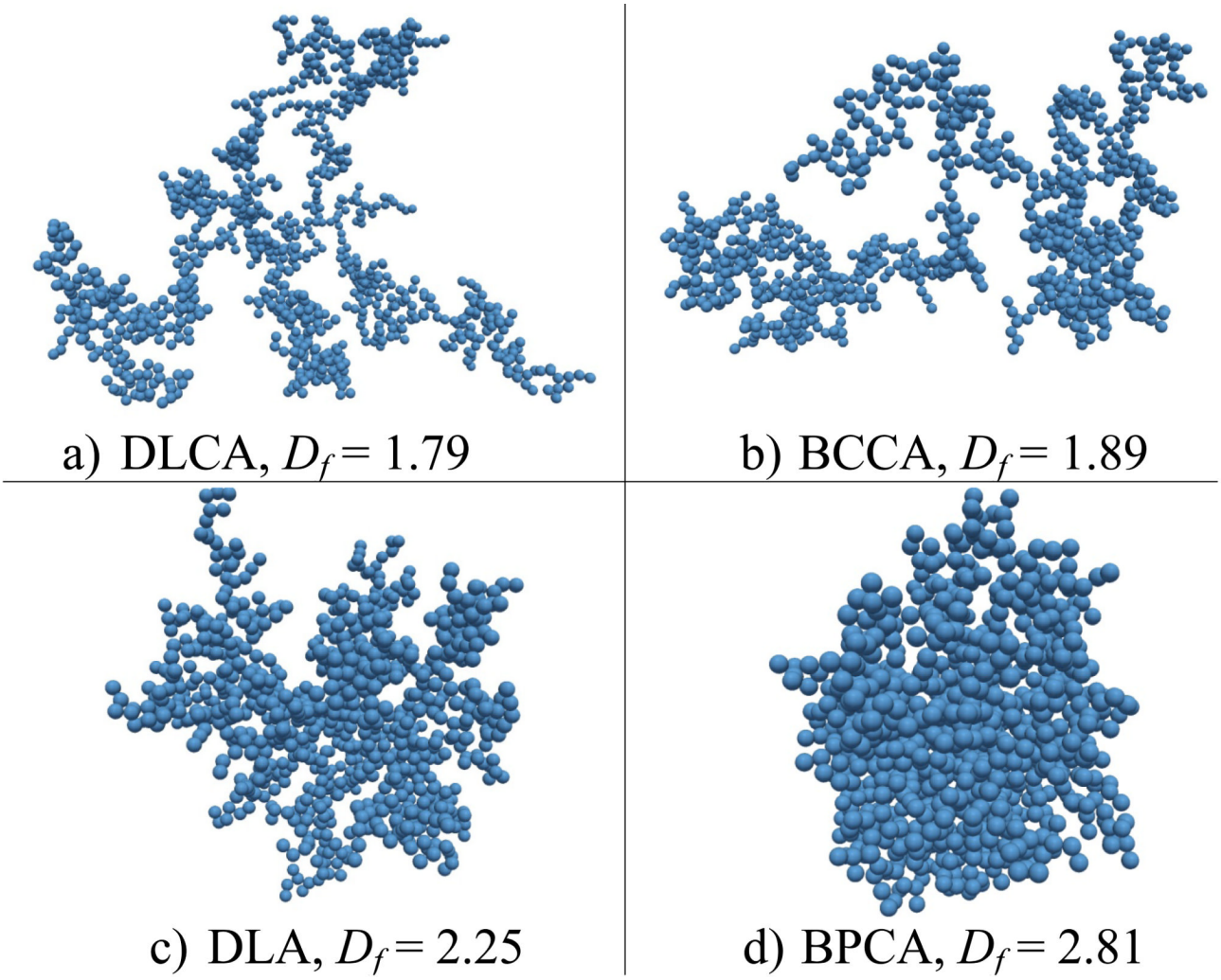

Figure 1.
Agglomerates consisting of 1024 monodisperse primary particles made by a) diffusion-limited (DLCA) and b) ballistic cluster-cluster (BCCA) agglomeration as well as by c) diffusion-limited (DLA) and d) ballistic particle-cluster (BPCA) agglomeration. These agglomerates have D_f = 1.79, 1.89, 2.25 and 2.81 identical to those calculated by Botet et al. (1982), Tence et al. (1986), Witten and Sander (1981) and Sutherland (1966), respectively.

Europe PMC Funders Author Manuscripts

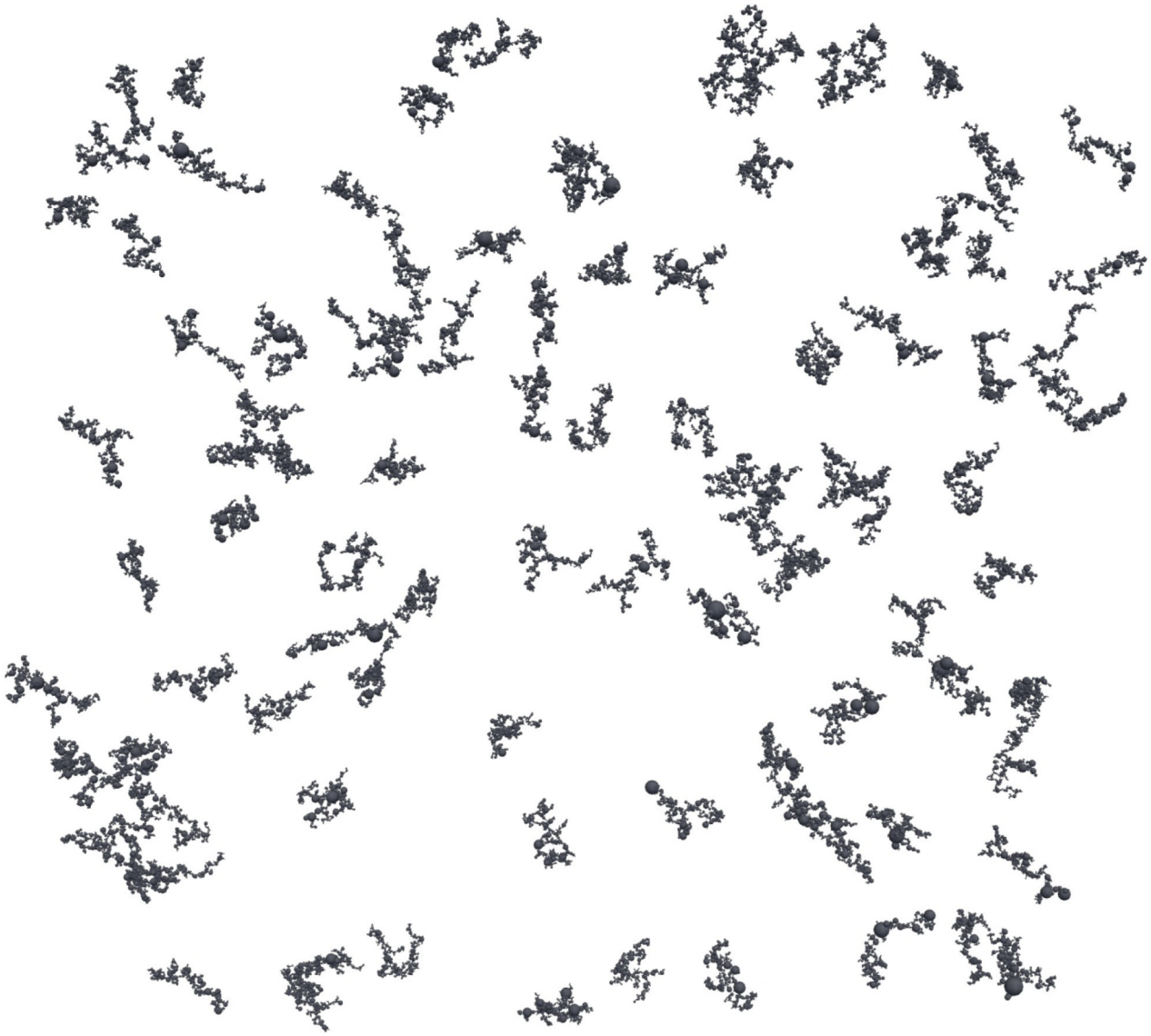

Figure 2.
Snapshot of 100 agglomerates made by diffusion-limited cluster-cluster agglomeration (DLCA) consisting of 512 primary particles with a log-normal size distribution with geometric standard deviation $\sigma_g = 2$.

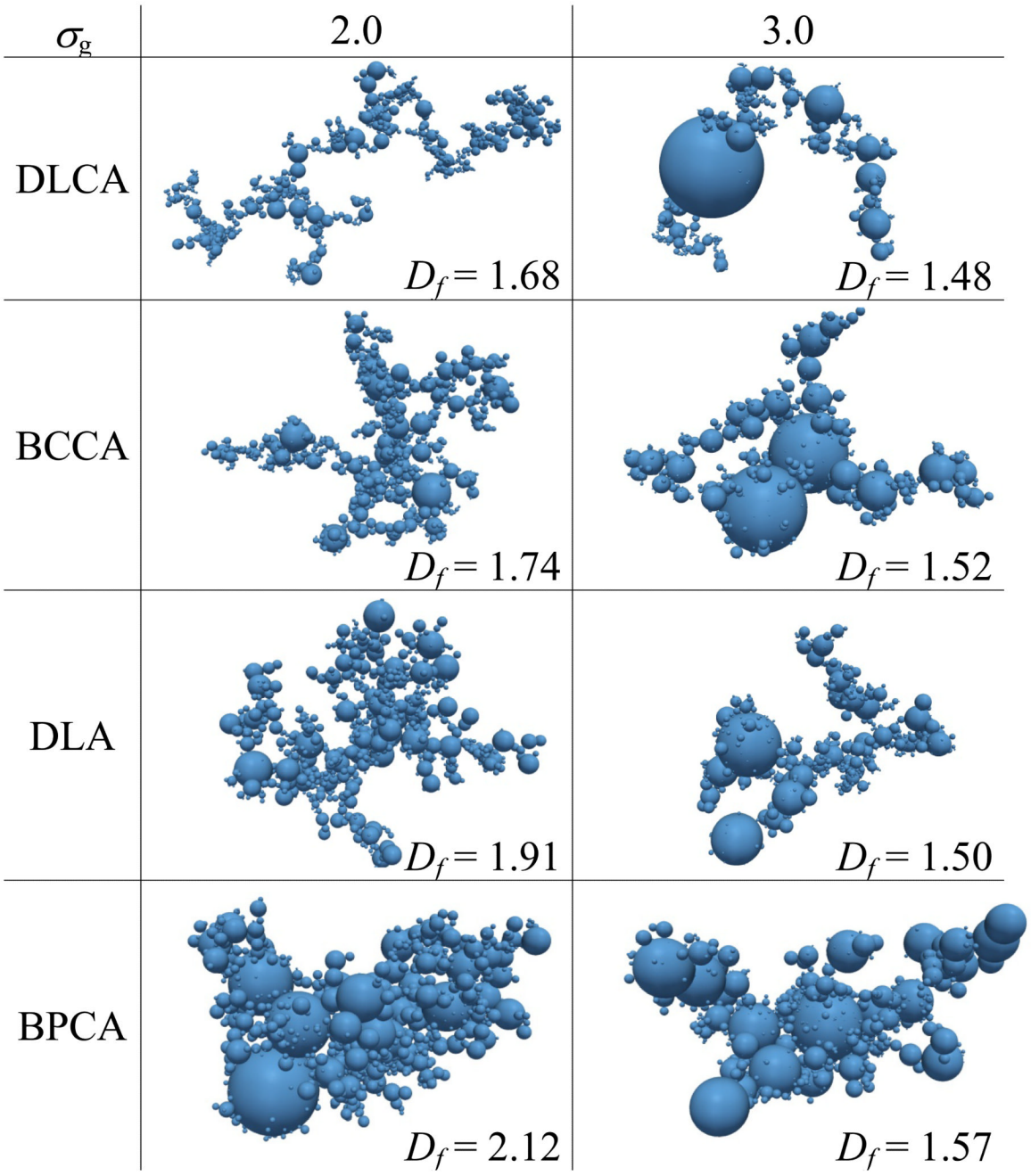

Figure 3.
Agglomerates of polydisperse primary particles having geometric standard deviation σ_g = 2.0 (left column) and 3.0 (right column) made by diffusion-limited (DLCA) and ballistic cluster-cluster agglomeration (BCCA) as well as diffusion-limited (DLA) and ballistic particle-cluster agglomeration (BPCA). The structure of agglomerates consisting of very polydisperse (σ_g = 3) particles is quite similar (D_f = 1.48 – 1.57) indicating that their polydispersity essentially "washes out" differences in agglomeration mechanisms.

Europe PMC Funders Author Manuscripts

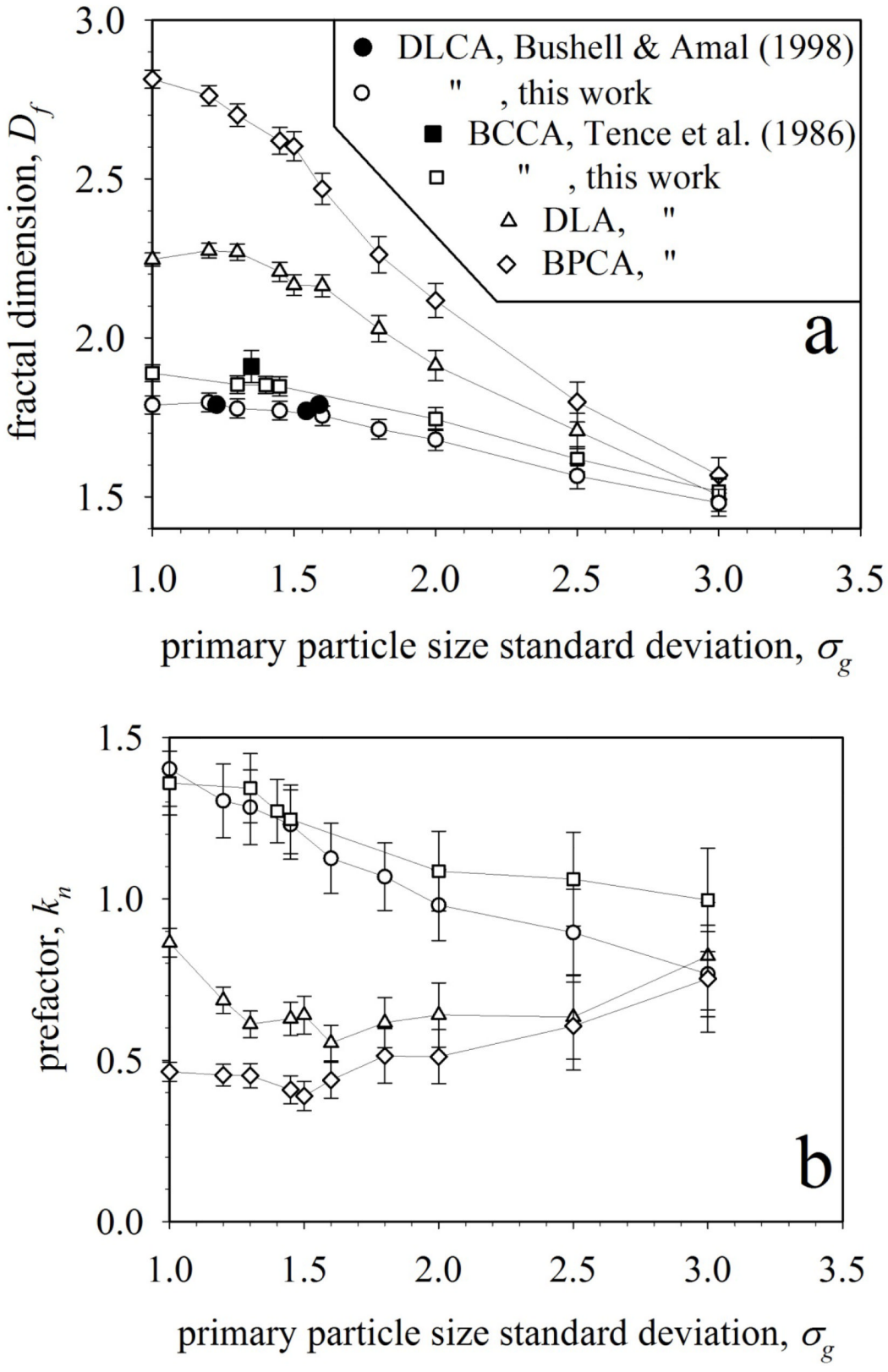

Figure 4.

The asymptotic (a) fractal dimension D_f and (b) prefactor k_n of 500 agglomerates as a function of the geometric standard deviation, σ_g, of their primary particles (PP) for different collision or agglomeration mechanisms. At $\sigma_g = 1$ (monodisperse PP) the classic D_f of the corresponding structures are obtained. With increasing σ_g, the D_f decreases gradually reaching asymptotically ≈ 1.5 (a) and $k_n \approx 1$ (b) at $\sigma_g = 3$, nearly independent of agglomeration mechanism.

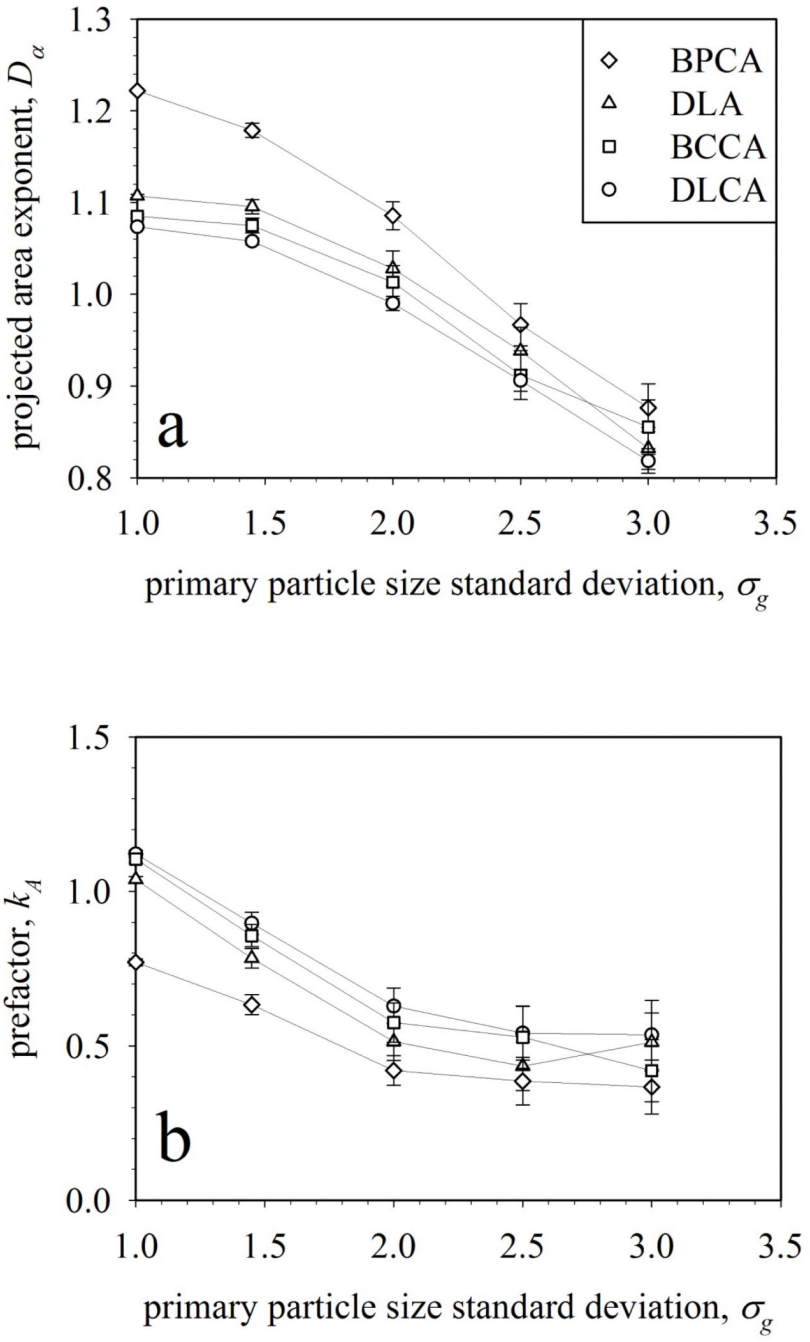

Figure 5.
The projected area exponent D_α (a) and prefactor k_a (b) of DLCA (circles), BCCA (squares), DLA (triangles) and BPCA (diamonds) agglomerates as a function of the geometric standard deviation σ_g of their constituent primary particles. The D_α and k_a decrease monotonically for increasing σ_g regardless of agglomerate generation mechanism.

Europe PMC Funders Author Manuscripts

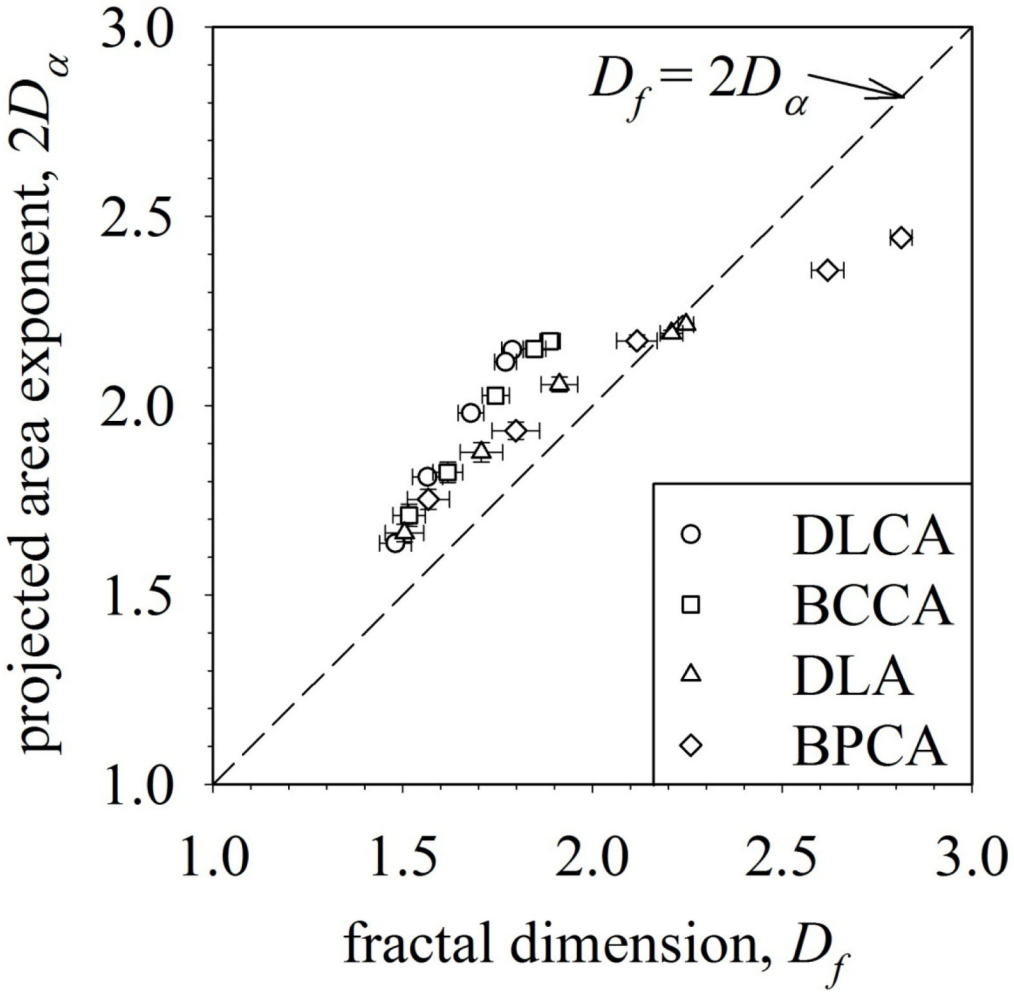

Figure 6.
The fractal dimension D_f versus projected area exponent $2D_a$ for DLCA (circles), BCCA (squares), DLA (triangles) and BPCA (diamonds) agglomerates and σ_g = 1-3. The broken line corresponds to $D_f = 2D_a$. For cluster-cluster agglomerates $2D_a$ is always larger than D_f, while particle-cluster agglomerates have a transition at $D_f \approx 2.1$ between σ_g = 1.5 and 2.

Table 1

The prefactor k_n and fractal dimension D_f of agglomerates made by DLCA, BCCA, DLA and BPCA as obtained using the actual PP number n_p and radius r_p are compared to k_n and D_f obtained assuming monodisperse PPs of equivalent average number n_{va} and radius r_{va} (eq. 3 & 4).

σ_g	D_f	k_n	D_f	k_n
	Actual n_p and r_p		Monodisperse assumption, n_{va} & r_{va} (eq. 3 & 4)	
	DLCA			
1.00	1.79 ± 0.03	1.40 ± 0.12	1.79 ± 0.03	1.40 ± 0.12
1.45	1.77 ± 0.03	1.23 ± 0.11	1.79 ± 0.03	1.42 ± 0.11
2.00	1.68 ± 0.03	0.98 ± 0.11	1.74 ± 0.03	1.53 ± 0.11
2.50	1.57 ± 0.04	0.90 ± 0.13	1.68 ± 0.04	1.66 ± 0.11
3.00	1.48 ± 0.04	0.77 ± 0.13	1.60 ± 0.04	1.80 ± 0.11
σ_g	BCCA			
1.00	1.89 ± 0.03	1.36 ± 0.10	1.89 ± 0.03	1.36 ± 0.10
1.45	1.85 ± 0.03	1.25 ± 0.11	1.86 ± 0.03	1.49 ± 0.11
2.00	1.74 ± 0.04	1.09 ± 0.12	1.75 ± 0.03	2.04 ± 0.14
2.50	1.62 ± 0.04	1.06 ± 0.15	1.53 ± 0.04	3.01 ± 0.19
3.00	1.52 ± 0.04	1.00 ± 0.16	1.36 ± 0.04	3.62 ± 0.20
σ_g	DLA			
1.00	2.25 ± 0.02	0.86 ± 0.04	2.25 ± 0.02	0.86 ± 0.04
1.45	2.21 ± 0.03	0.63 ± 0.05	2.21 ± 0.03	0.83 ± 0.05
2.00	1.91 ± 0.05	0.64 ± 0.10	1.91 ± 0.05	1.23 ± 0.10
2.50	1.71 ± 0.06	0.63 ± 0.13	1.71 ± 0.06	1.50 ± 0.13
3.00	1.51 ± 0.05	0.82 ± 0.17	1.51 ± 0.05	2.31 ± 0.2
σ_g	BPCA			
1.00	2.81 ± 0.03	0.46 ± 0.03	2.81 ± 0.03	0.46 ± 0.03
1.45	2.62 ± 0.04	0.41 ± 0.04	2.70 ± 0.04	0.55 ± 0.04
2.00	2.12 ± 0.05	0.51 ± 0.08	2.26 ± 0.05	1.17 ± 0.11
2.50	1.80 ± 0.06	0.61 ± 0.14	1.93 ± 0.06	1.76 ± 0.17
3.00	1.57 ± 0.06	0.75 ± 0.17	1.58 ± 0.06	2.56 ± 0.21